Paper:
Wint, N., McMurray, H., Williams, G. & de Vooys, A. (2016). The Kinetics and Mechanism of Atmospheric Corrosion Occurring on Tin and Iron-Tin Intermetallic Coated Steels. *Journal of The Electrochemical Society, 163*(2), C1-C6.
http://dx.doi.org/10.1149/2.1081514jes

The Kinetics and Mechanism of Atmospheric Corrosion Occurring on Tin and Iron-Tin Intermetallic Coated Steels

II. Filiform Corrosion

N. Wint,[a,z] H. N. McMurray,[a,*] G. Williams,[a] and A. C. A. de Vooys[b]

[a]*Materials Research Centre, College of Engineering, Swansea University, Bay Campus, Swansea, SA1 8EN, United Kingdom*
[b]*Tata Steel Research and Development, 1970 CA IJmuiden, The Netherlands*

This paper describes a systematic study into the initiation and propagation of filiform corrosion (FFC) on pure iron, pure tin and industrially important tin and iron-tin intermetallic (FeSn and $FeSn_2$) coatings for packaging steels, as a function of coating weight. The time-dependent extent of FFC was determined optically. FFC was not observed on pure tin or tin coatings but was found to propagate at significantly reduced rates on the FeSn and $FeSn_2$ intermetallic coatings, when compared to pure iron. An explanation of the findings is given, firstly, in terms of the open circuit potential (OCP) and the extent to which polarity of the galvanic corrosion cell formed between relevant phases permits FFC propagation, and secondly in terms of the relative susceptibility of the various phases to anodic dissolution. It is concluded that even when FFC is feasible thermodynamically, propagation rates may be negligible due to the low activity for anodic dissolution of tin and iron-tin intermetallics.
 [DOI: 10.1149/2.1081514jes] All rights reserved.

Manuscript submitted September 2, 2015; revised manuscript received October 19, 2015. Published October 29, 2015. This was Paper 796 presented at the Cancun, Mexico, Meeting of the Society, October 5–9, 2014.

The increasing price of tin in the commodities market has resulted in a need to reduce the amount of tin used in tinplate materials (tin coating weight) for the corrosion protection of packaging steel whilst retaining adequate corrosion resistance.[1]

One approach to doing this has been to diffusion anneal the unflowed tin ($<1 g.m^{-2}$) in a reducing atmosphere at temperatures above 500°C[2,3] in such a way that almost all (preferably 90–98%)[4] of the free tin is converted to an iron-tin (FeSn) intermetallic as discussed during Part 1 of this paper.[1]

The aim of the current paper is to present a detailed study of the role of free tin and iron-tin intermetallic layers in resisting atmospheric corrosion, specifically filiform corrosion (FFC), as it affects the external surface of lacquer coated packaging material.

FFC, which produces 'threadlike' corrosion product deposits, tends to propagate from breaks or penetrative defects in organically coated metal products. It is widely accepted that filament advance involves anodic undercutting at the 'active head.' This process is driven by differential aeration arising from facile O_2 diffusion in the filament tail, which consists of dry corrosion products as shown by schematic a of Figure 1 [5–11]. Elsewhere it has been suggested that delamination of the protective layer from the substrate is due to cathodic mechanisms in the vicinity of the head.[12] Senöz et al. used SKPFM to show that the anodic reaction within the head drives cathodic delamination of the coating at intermetallic particles within aluminum alloys. It was subsequently concluded that the particles within the vicinity of the head determined the direction of FFC[13,14] Williams and McMurray observed an area of cathodic delamination proceeding the head but contest its function as a primary cathode, claiming it plays no role in the mechanism of FFC advance.[15]

FFC has previously been observed on exposed steel on score lines of packaging material lids, causing perforations from the outside in.[16,17] Morita and Yoshida studied the FFC behavior of lightly tin-coated steel for welded cans in relation to free tin, where free tin coating weight was defined as total tin minus alloyed tin.[18] However, their results were complicated by the presence of a chromium based coating.

Here the time-dependent extent of FFC on a range of technologically important tin and iron-tin intermetallic coated packaging steels has been investigated optically and electrochemically. An explanation of the findings is given, firstly, in terms of the galvanic polarity of the corrosion cell formed between relevant phases and secondly in terms of the relative susceptibility of the various phases to anodic dissolution.

Experimental

Materials.— Iron foil of 0.15 mm thickness and 99.5% purity and tin foil of 0.25 mm thickness and 99.8% purity were obtained from Goodfellow Cambridge Ltd. Mild steel with three different types of tin based coating were obtained from Tata Steel Packaging. The first coating consisted of unflowed porous pure tin of coating weight 2.8 $g.m^{-2}$. The second coating consisted of reflowed FeSn present at coating weights 0.44 $g.m^{-2}$ and 0.88 $g.m^{-2}$. The third coating was again reflowed and consisted of $FeSn_2$. The $FeSn_2$ coating was found to contain a small amount of surface free tin which was removed electrochemically by applying a controlled anodic current density in a 1 M HCl electrolyte[19,20]. The final $FeSn_2$ coating weights were calculated as 0.37 $g.m^{-2}$ and 1.6 $g.m^{-2}$ using chronocoulometry.

Polyvinyl butyral (PVB) and all other chemicals were obtained from Aldrich Chemical Co. and of analytical grade purity. All samples were cleaned and degreased using ethanol and distilled water before experimentation.

Methods.— In the case of electrochemical characterization experiments, coupons of approximately 40 mm x 30 mm were cut from large sheets to obtain a suitably sized sample. The sample was masked using extruded PTFE tape (type 5490 HD supplied by 3 M) which exposed a 10 mm × 10 mm area in the centre. Electrochemical measurements were taken using a Solartron 1280 Electrochemical Measurement Unit. A saturated calomel electrode (SCE) reference electrode was used to provide a fixed potential throughout the experiment. Open circuit potential (OCP) values were taken in a 0.1 M HCl electrolyte at 20°C. The electrolyte pH was typical of that found within a FFC head.[6,7,21] Potentiodynamic scans were conducted in a 0.6 $mol.dm^{-3}$ NaCl electrolyte at 20°C. Although the electrolyte pH was not representative of that within the FFC head it was considered that an acidic electrolyte would destroy samples. A platinum gauze counter electrode and a scan rate of 0.1667 $mV.sec^{-1}$ were used.

The initiation and propagation of FFC was investigated on five different materials as shown in Figure 1b and followed a methodology described elsewhere.[15] In the study of FFC on coated samples (Cell 3 – Cell 5) two types of sample were prepared. In the case of the first type the metallic coating was continuous. In the second type the metallic (tin or iron-tin intermetallic) coating was removed from

*Electrochemical Society Active Member.
[z]E-mail: 483404@swansea.ac.uk

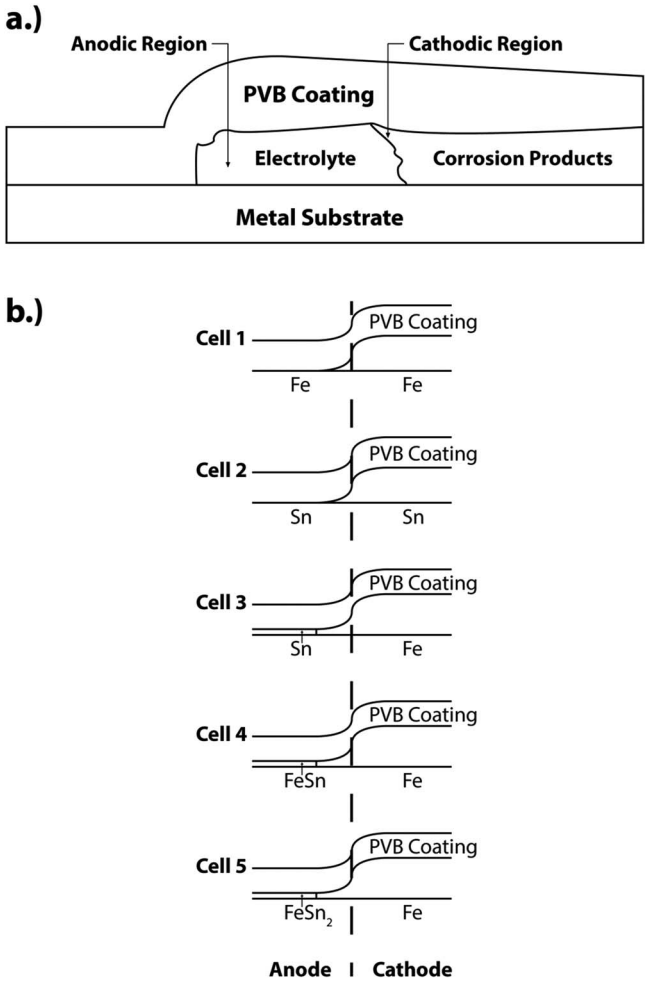

Figure 1. a.) Schematic showing filiform corrosion mechanism. b.) Schematics showing the five galvanic couples on which the initiation and propagation of filiform corrosion was investigated.

half the sample surface. All samples were then solvent coated with 15% w/w ethanolic solution of polyvinyl butyral (PVB), molecular weight 70,000–100,000, lacquer using insulating tape height guides to give an air-dried thickness of 30 μm. Two types of experiments were carried out. In the first type FFC was initiated on the coating. In the second type FFC was initiated on the exposed steel substrate and allowed to propagate over the coated portion of the sample. In all cases a 10 mm line penetrative PVB coating defect was created by scribing the sample with a scalpel blade. FFC was initiated by introducing 2 μL of 2.5×10^{-3} M aqueous $FeCl_2$ evenly over the length of the scribe using a glass microcapillary. After allowing the $FeCl_2$ to react with the exposed metal, and excess water to evaporate in air, samples were placed in an environmental chamber. The temperature was constant at 20°C and a relative humidity of 93% RH was maintained throughout the experiment by allowing the atmosphere to remain in equilibrium with a reference solution comprising saturated aqueous $Na_2SO_410H_2O$. Samples were removed from the humidity chamber at intervals in time to carry out photography and computerized image analysis. The image analysis software (Sigma Scan Pro) was calibrated by specifying a pre-measured distance between two points and inputting real distance. The surface area of the FFC attack was measured as that occupied by corrosive discoloration. A value for a designated surface area was then given and the rate of propagation calculated. Six repeat experiments were conducted for each material and confidence limits (errors) correspond to ± one unit of standard deviation on the mean rate value. Optical micrographs of FFC were obtained using a Keyence VHX-700F digital microscope.

Focused ion beam (FIB) milling was used to investigate a cross section of the FeSn coated sample to determine whether removal of the coating occurred during FFC propagation. The instrument used was a FEI Strata FIB 200 × P. A shallow trench was cut using a gallium ion beam and a standard cross section pattern ~25 μm × 15 μm and ~ 10–15 μm deep. The trench face was cleaned using a beam of lower beam current. The sample was tilted by approximately 45° for imaging.

Table I. Free Corrosion Potential of pure iron, pure tin and FeSn and $FeSn_2$ intermetallic coatings in 0.1 M HCl at 20°C.

Material	E_{corr} (V vs. SHE)
Pure Tin	-0.262 ± 0.0041
$FeSn_2$	-0.292 ± 0.0021
FeSn	-0.296 ± 0.0047
Pure Iron	-0.320 ± 0.0081

Results and Discussion

Electrochemical characterization.—OCP characterization Results.— All materials were characterized in terms of their OCP at 20°C in a 0.1 M HCl electrolyte, the results being shown in Table I. The confidence limits (errors) shown correspond to ± one unit of standard deviation on the mean, on the basis of three repeat measurements.

Potentiodynamic results.—Potentiodynamic scans were conducted in a 0.6 $mol.dm^{-3}$ NaCl electrolyte at 20°C. A scan rate of 0.1667 $mV.sec^{-1}$ was used and results are shown in Figure 2. Figure 2 shows that anodic currents measured on FeSn are over ten times smaller than those observed for pure iron at the potential value ~ 0 V vs. SHE. FeSn therefore has a significantly higher anodic overpotential near open circuit potential values. Pure tin achieves passivity fairly rapidly over this range of potentials; breakdown occurs at values of ~−0.25 V vs. SHE. In comparison the overpotential to achieve passivity on pure iron or FeSn is much higher. The three zero current measurements observed in the case of iron indicates an active/passive transition suggesting the material is unstable, this being expected at the relevant pH.[22]

Filiform results.—Pure iron cell (Cell 1).—FFC was observed on pure iron when initiated using a 0.0025 M $FeCl_2$ electrolyte. This finding is in agreement with the literature, the term 'filiform corrosion' first being used by Sharman in 1944 when studying lacquered steel surfaces.[7,15,21] The catalytic properties of iron with respect to the oxygen reduction reaction (ORR) have been demonstrated during Part 1

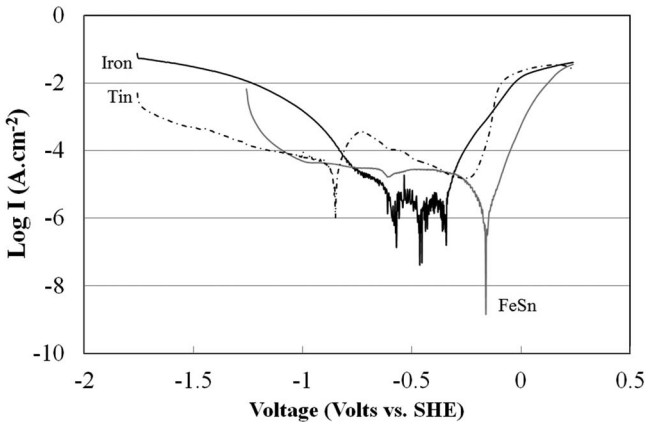

Figure 2. Current density as a function of potential in aerated 0.6 $mol.dm^{-3}$ NaCl. Potential sweep rate 0.1667×10^{-3} Vs^{-1}.+.

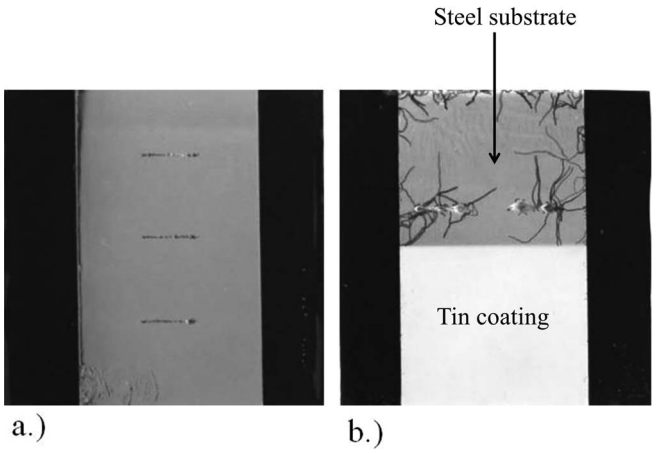

Figure 3. Photographs of samples taken after 6 weeks showing that a.) FFC could not be initiated on tin coated steel and b.) FFC did not propagate into tin coated steel when initiated on a steel substrate, using 0.0025 M $FeCl_2$.

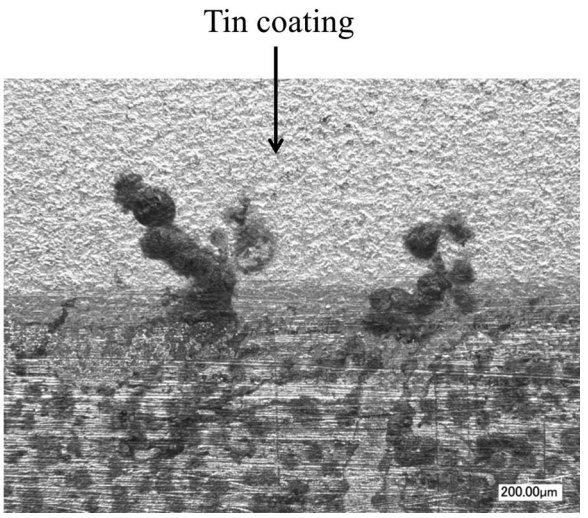

Figure 4. An optical microscope image showing the propagation of FFC onto the intact tinplate region from the steel substrate on which it was initiated using 0.0025 M $FeCl_2$.

of this paper and previously.[1,23,24] The material is capable of maintaining an acidic electrolyte, the pKa for Fe (III) being 2.2, and is active at the relevant pH values.[22]

Pure tin cell (Cell 2).—FFC was not observed to occur on pure tin when initiated using a 0.0025 M $FeCl_2$ electrolyte. The pKa for Sn (II) is 3.4 and Sn (IV) 2.2.[25] In theory, the head electrolyte is therefore acidic enough for FFC to be maintained and it is thus suggested that there is alternative reason that FFC is not observed. Tin is also active at the pH relating to that within the head electrolyte.[22] With respect to the cathodic reaction, it has been stated that tin is associated with a high oxygen overpotential elsewhere.[26] This is confirmed by results given during Part 1 of this paper which confirms a high overpotential of pure tin with respect to the ORR, when compared to pure iron and the FeSn and $FeSn_2$ intermetallic coatings.[1]

Tin-Iron cell (Cell 3).—The visual appearance of tin coated steel of both experimental types, 6 weeks after initiation, are shown in Figure 3.

As can be seen**,** FFC was not initiated on the tin coating. This supports the work of Morita and Yoshida who found that FFC was retarded by high cathodic polarization with increasing levels of free tin.[18] The Keyence VHX-700F digital microscope was used to acquire images of the boundary between the steel and intact tinplate region as shown in Figure 4. FFC was found to propagate <500 µm when initiated on the steel substrate.

OCP characterization shows that pure tin is not sacrificial to iron at pH 1, this being typical of that found within the FFC head.[6,7,21] It has previously been found that the relative potential of tin and iron can be altered by the presence of pure acid and food media in which organic acids (carboxylic) form stable complexes (SnL) with Sn^{2+} and/or Sn^{4+} ions.[27–29] However, in the present case the galvanic polarity of the iron-tin cell ensures the FFC does not propagate farther into the tinplate and remains on the steel substrate

FeSn-iron cell (Cell 4) and $FeSn_2$–iron cell (Cell 5).—FFC corrosion has previously been found to accelerate on $FeSn_2$ in the presence of free tin due to galvanic coupling and the formation of microcells.[18] These results were however made more complex by the presence of an additional chromium/chromium oxide coating.[18] In the present case FFC has been shown to occur in the absence of both free tin and chromium. Figure 5 and Figure 6 show that FFC was both initiated on 0.44 $g.m^{-2}$ FeSn and propagated onto 0.44 $g.m^{-2}$ FeSn after ini-

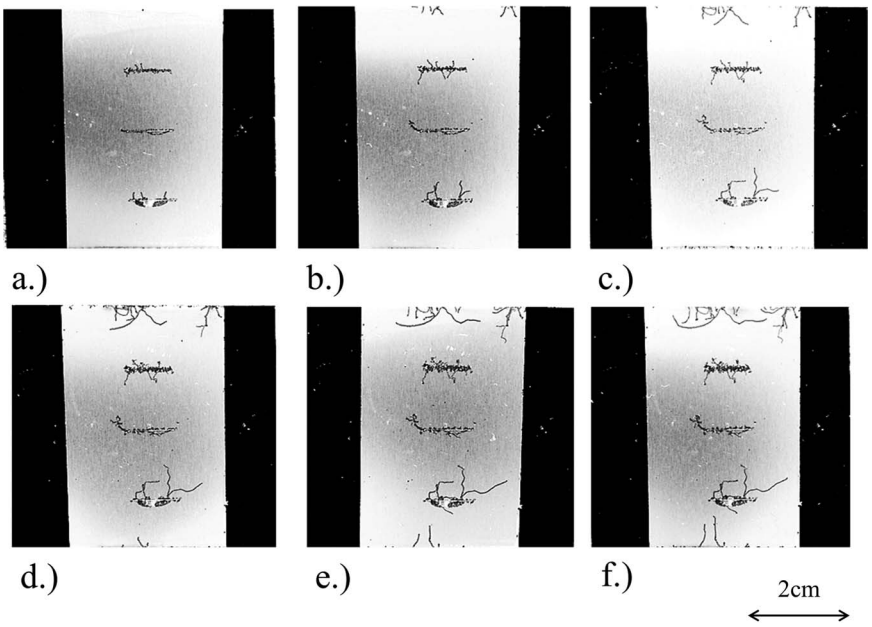

Figure 5. Photographs of samples taken a.) 1 week, b.) 2 weeks, c.) 3 weeks, d.) 4 weeks, e.) 5 weeks and f.) 6 weeks after initiation showing that FFC could be initiated on 0.44 $g.m^{-2}$ FeSn using 0.0025 M $FeCl_2$.

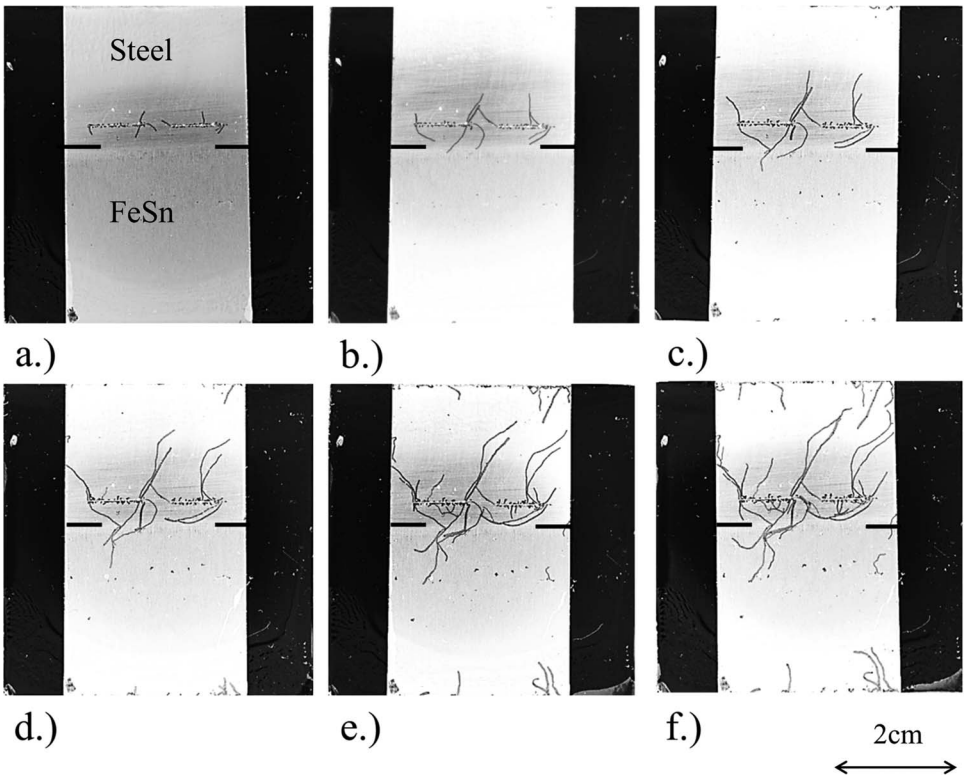

Figure 6. Photographs of samples taken a.) 1 week, b.) 2 weeks, c.) 3 weeks, d.) 4 weeks, e.) 5 weeks and f.) 6 weeks after initiation showing that FFC could propagate onto 0.44 g.m^{-2} FeSn after initiation on the steel substrate using 0.0025 M $FeCl_2$.

tiation on the steel substrate using 0.0025 M $FeCl_2$. Figure 7 shows a comparison between FFC on 0.44 g.m^{-2} and 0.88 g.m^{-2} FeSn, 6 weeks after initiation. In the case of the former sample substantially more corroded area exists. Figure 8 shows images of FFC initiated on 0.37 g.m^{-2} $FeSn_2$.

The increase in corroded area with decrease in coating weight is supported by Figures 9a and 9b, which show the linear growth rate of the sample area over which coating delamination had occurred as determined by image analysis of pure iron and FeSn and $FeSn_2$ intermetallic coatings over the experimental time periods. The linear growth rate was found to be (0.0353 ± 0.0032) mm^2.hr^{-1} on 0.44 g.m^{-2} FeSn, and (0.0122 ± 0.0011) mm^2.hr^{-1} on 0.88 g.m^{-2} FeSn, in comparison to (0.0551 ± 0.0050) mm^2.hr^{-1} on iron. The linear growth rate was found to be (0.0296 ± 0.0027) mm^2.hr^{-1} on 0.37 g.m^{-2} $FeSn_2$, and (0.012 ± 0.0011) mm^2.hr^{-1} on 1.6 g.m^{-2} $FeSn_2$. The confidence limits (errors) shown correspond to ± one unit of standard deviation on the mean based on six measurements. For both intermetallics**,** the rate of FFC decreases with increasing intermetallic coating weight. It is therefore suggested that the coating acts as a barrier and in order for the FFC to progress forward the coating must be dissolved, thus exposing the iron substrate which, as shown

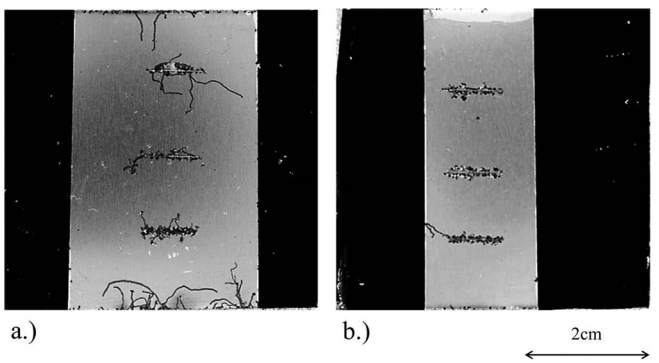

Figure 7. Photographs of samples taken after 6 weeks comparing FFC initiated on a.) 0.44 g.m^{-2} FeSn and b.) 0.88 g.m^{-2} FeSn coated steel, using 0.0025 M $FeCl_2$.

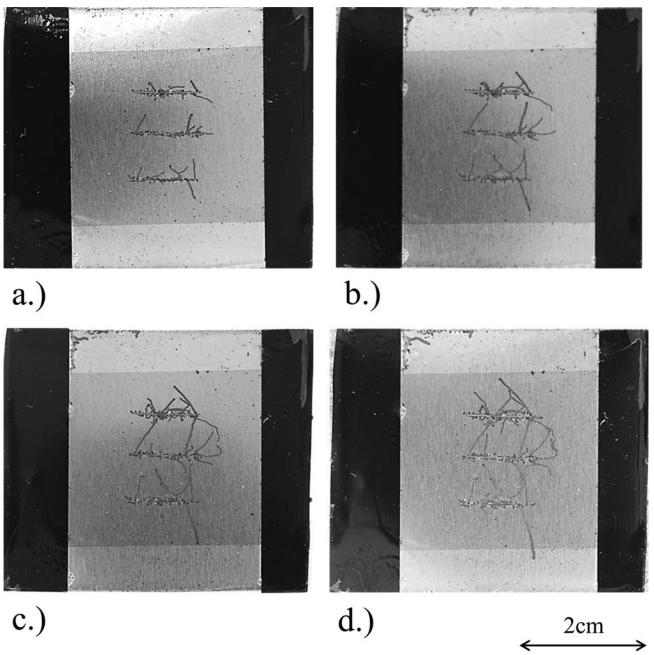

Figure 8. Photographs of samples taken after a.) 1 week, b.) 2 weeks, c.) 3 weeks and d.) 4 weeks showing that FFC could be initiated on 0.37 g.m^{-2} $FeSn_2$ using 0.0025 M $FeCl_2$.

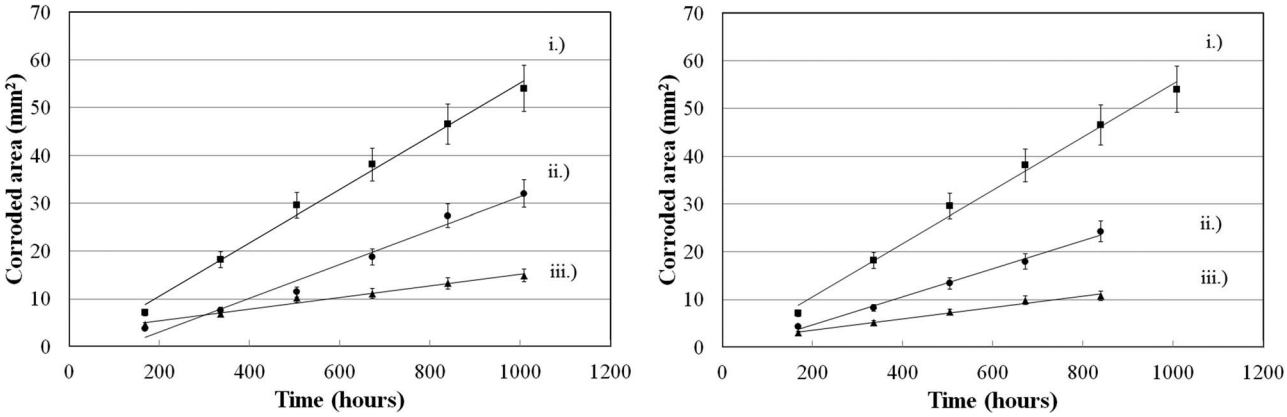

Figure 9. Graph showing the corroded area after the initiation of FFC using 0.0025 M $FeCl_2$ on PVB coated ai.) pure iron ii.) 0.44 g.m^{-2} FeSn and iii.) 0.88 g.m^{-2} FeSn bi.) pure iron and ii.) 0.37 g.m^{-2} $FeSn_2$ and iii.) 1.6 g.m^{-2} $FeSn_2$ coated steel.

previously, is a strong electrocatalyst for the ORR and thus becomes the cathode.[1,23,24] In the case of higher coating weights, increased currents are needed for longer periods of times in order for FFC to propagate, thus leading to a reduced rate. This theory is consistent with images obtained using FIB, during which the sample was initially milled after applying a platinum layer which acted as a protective sacrificial barrier. Figure 10a shows the intact coating, and Figure 10b a cross section within the tail region. As can be seen the anodic attack of the coating does not stop on the intermetallic, but continues into the substrate.

The E_{corr} of FeSn and $FeSn_2$ was found to be 0.024 V and 0.028 V higher than that of pure iron, respectively. The small difference in values for both couples renders FFC thermodynamically feasible. It is therefore considered that the reduced propagation rate of FFC, when compared to iron, is due to the low electrocatalytic activity of FeSn with respect to anodic dissolution as shown in Figure 2. Whereas tin achieves passivity fairly rapidly causing a reduction in corrosion rate, no passivity is seen on pure iron or FeSn over the range of potentials investigated and thus their rate of anodic dissolution is higher.

The rate of FFC propagation was found to be identical, 0.012 mm^2.hr^{-1}, on both 0.88 g.m^{-2} FeSn and 1.6 g.m^{-2} $FeSn_2$. It is thus suggested that a higher coating weight is needed in the case of $FeSn_2$ to resist FFC to the same extent as FeSn. It is widely reported that there is no obvious mass transport limitation on FFC propagation and kinetics are suggested to be surface controlled.[6,7,11] It is therefore proposed that the greater true surface area of $FeSn_2$, as described during Part 1 of this paper, allows greater kinetic currents and thus FFC propagation rates are increased[1].

Conclusions

A systematic optical and electrochemical study has been completed to show that;

- Filiform corrosion (FFC) could not be initiated on pure tin.
- FFC was not observed to initiate on steel coated with unflowed pure tin.
- FFC was observed on both FeSn and $FeSn_2$, propagation rates being lower than that on pure iron and decreasing with increasing coating weight in both cases.
- Corrosion of both intermetallic and underlying substrate occurs during the FFC of FeSn.

An electrochemical study has been completed to show that;

- Pure tin was not sacrificial to pure iron at the relevant pH 1.
- FeSn and $FeSn_2$ intermetallics were not sacrificial to pure iron at pH 1.

It is proposed that;

- In all cases wholly or partially exposed iron substrate acts cathodically.
- The galvanic polarity of the iron-tin cell created did not permit the propagation of FFC at the corresponding pH.
- During the FFC of the FeSn and $FeSn_2$ intermetallic coated steel the coatings became the site of anodic metal dissolution.

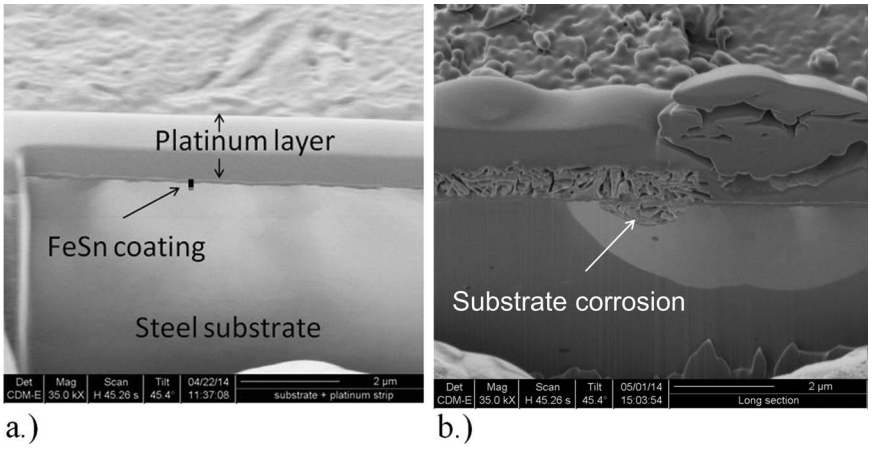

Figure 10. SEM image showing a.) intact FeSn coating and b.) substrate corrosion in a trench cut from a tail of FFC initiated on 0.88 g.m^{-2} FeSn.

- The reduction in FFC propagation rate on FeSn and $FeSn_2$, when compared to iron, was due to the low activity of tin and iron-tin intermetallics for anodic dissolution.

Acknowledgments

The authors would like to thank the European Social Fund (ESF) through the Welsh Government for the financial support of the Steel Training Research and Innovation Partnership (STRIP). In addition, the support from TATA Steel is gratefully acknowledged. Andrew Dyer of Cranfield University is kindly thanked for acquisition of FIB images.

References

1. N. Wint, S. Geary, H. N. McMurray, and A. C. A. de Vooys, The Kinetics and Mechanism of Atmospheric Corrosion Occurring on Tin and Iron-Tin Intermetallic Coated Steels: Part 1 Cathodic Delamination. *Journal of the Electrochemical Society*, **162**, C775 (2015).
2. M. Fujinami, K. Yoshida, Y. Ujihira, and M. Terasaka, *Journal of Materials Science*, **20**, 4099 (1985).
3. H. Kuroda, I. Onoda, T. Inui, and Y. Kondo, *Characteristics of Lightly Tin Coated Steel Sheets*, p.124, *The Proceedings of the Second International Tinplate Conference*, London (1980).
4. I. Portegies Zwart and J. H. O. J. Wijenberg, Tata Steel Ijmuiden, *Process for producing an iron-tin layer on a packaging steel substrate*, Patent WO 2012/045791, 12 April, 2012.
5. G. Williams and H. N. McMurray, in *Shreir's Corrosion*, B. R. A. Cottis, M. Graham, R. Lindsay, S. Lyon, T. J. A. Richardson, D. J. D. Scantlebury, and H. Stott, Editors, p. 988, Elsevier Science (2009).
6. A. Bautista. *Progress in Organic Coatings*, **28**, 49 (1996).
7. R. T. Ruggeri and T. R. Beck, *Corrosion-NACE*, **39**, 452 (1983).
8. W. Schmidt and M. Stratmann, *Corrosion Science*, **40**, 1441 (1998).
9. G. Grundmeier, W. Schmidt, and M. Stratmann, *Electrochimica Acta*, **45**, 2515 (2000).
10. J. H. W. de Wit, *Electrochimica Acta*, **46**, 3641 (2001).
11. T. M. Watson, A. J. Coleman, G. Williams, and H. N. McMurray, *Corrosion Science*, **89**, 46 (2014).
12. W. Funke, *Industrial and Engineering Chemistry Product Research and Development*, **24**, 343 (1985).
13. C. Senöz, S. Borodin, M. Stratmann, and M. Rohwerder, *Corrosion Science*, **58**, 307 (2012).
14. C. Senöz and M. Rohwerder, *Electrochimica Acta*, **56**, 9588 (2011).
15. G. Williams and H. N. McMurray, *Electrochemistry Communications*, **5**, 871 (2003).
16. J. E. Charbonneau, *Scanning*, **23**, 198 (2001).
17. J. E. Charbonneau, *Scanning*, **19**, 512 (1997).
18. J. Morita and M. Yoshida, *Corrosion-NACE*, **50**, 11 (1994).
19. American Society for Testing and Materials, *Standard Test Methods for Determination of Tin Coating Weights for Electrolytic Tinplate*, A 630–98, 4 (1998).
20. A. Ninčević Grassino, Z. Grabarić, A. Pezzani, G. Fasanaro, and A. Lo Voi, *Food and Chemical Toxicology*, **47**, 1556 (2009).
21. G. M. Hoch, in *Localized Corrosion*, R. W. Staehle, B. F. Brown, J. Kruger, and A. Agrawal, Editors, p.134, NACE International, Houston, TX (1974).
22. M. Pourbaix, *Atlas of Electrochemical Equilibria in Aqueous Solutions*, Pergamon Press (1966).
23. V. Jovancicevic and J. O'M. Bockris, *Journal of the Electrochemical Society*, **133**, 1797 (1986).
24. H. Dafydd, D. A. Worsley, and H. N. McMurray, *Corrosion Science*, **47**, 3006 (2005).
25. J. Burgess, *Metal Ions in Solution*, Ellis Horwood Limited, Chichester (1978).
26. I. A. Ammar, S. Darwish, M. W. Khalil, and A. Galal, *Z. Werkstofftech*, **16**, 194 (1985).
27. A. R. Willey, *British Corrosion Journal*, **7**, 29 (1972).
28. M. S. Abdel-Aal and M. H. Wahdan, *British Corrosion Journal*, **23**, 25 (1988).
29. T. P. Hoar, *Transactions of the Faraday Society*, **30**, 472 (1934).